Significance of Na/Ca Exchange for Ca^{2+} Buffering and Electrical Activity in Mouse Pancreatic β-Cells

David Gall,* Jesper Gromada,# Isabella Susa,§ Patrik Rorsman,¶ André Herchuelz,* and Krister Bokvist#

*Laboratoire de Pharmacodynamie et de Thérapeutique, Faculté de Médecine, Université Libre de Bruxelles, B-1070 Bruxelles, Belgium; #Islet Cell Physiology, Novo Nordisk A/S, DK-2880 Bagsvaerd, Denmark; §Service de Chimie Physique, Faculté des Sciences, Université Libre de Bruxelles, B-1050 Bruxelles, Belgium; and ¶Department of Physiology and Neuroscience, Lund University, S-223 62 Lund, Sweden

ABSTRACT   We have combined the patch-clamp technique with microfluorimetry of the cytoplasmic Ca^{2+} concentration ([Ca^{2+}]$_i$) to characterize Na/Ca exchange in mouse β-cells and to determine its importance for [Ca^{2+}]$_i$ buffering and shaping of glucose-induced electrical activity. The exchanger contributes to Ca^{2+} removal at [Ca^{2+}]$_i$ above 1 μM, where it accounts for >35% of the total removal rate. At lower [Ca^{2+}]$_i$, thapsigargin-sensitive Ca^{2+}-ATPases constitute a major (70% at 0.8 μM [Ca^{2+}]$_i$) mechanism for Ca^{2+} removal. The β-cell Na/Ca exchanger is electrogenic and has a stoichiometry of three Na$^+$ for one Ca^{2+}. The current arising from its operation reverses at $\sim$−20 mV (current inward at more negative voltages), has a conductance of 53 pS/pF (14 μM [Ca^{2+}]$_i$), and is abolished by removal of external Na$^+$ or by intracellularly applied XIP (exchange inhibitory peptide). Inhibition of the exchanger results in shortening (50%) of the bursts of action potentials of glucose-stimulated β-cells in intact islets and a slight (5 mV) hyperpolarization. Mathematical simulations suggest that the stimulatory action of glucose on β-cell electrical activity may be accounted for in part by glucose-induced reduction of the cytoplasmic Na$^+$ concentration with resultant activation of the exchanger.

INTRODUCTION

In the presence of insulin-releasing glucose concentrations, the pancreatic β-cell generates a characteristic pattern of electrical activity that consists of oscillations between a depolarized plateau potential, on which action potentials are superimposed (= bursts), and repolarized electrically silent intervals (for review see Henquin and Meissner, 1984). The bursts of action potentials in the β-cell have been postulated to represent a long-lasting action potential with properties reminiscent of the cardiac action potential (Cook et al., 1980). Indeed, when the voltage-gated K$^+$ channels are blocked with tetraethylammonium, electrical activity in the β-cell consists of long-lasting action potentials strikingly similar to those encountered in the heart (Atwater et al., 1979; Santos and Rojas, 1989; Rorsman et al., 1992). In the cardiac myocyte, Na/Ca exchange is the major mechanism of Ca^{2+} extrusion, restoring basal Ca^{2+} levels between heartbeats (Bers, 1991). The cardiac Na/Ca exchange is electrogenic, with a stoichiometry of three Na$^+$ for one Ca^{2+} (Eisner and Lederer, 1985; Kimura et al., 1987; Ehara et al., 1989). The operation of the exchange thereby gives rise to an inward (depolarizing) current, which prolongs the depolarized plateau phase of the myocyte action potential (Egan et al., 1989; Noble et al., 1991). The Na/Ca exchanger was recently cloned from heart (Nicoll et al., 1990). Three genes coding for three different exchangers (NCX1, NCX2,

and NCX3) have been identified (Nicoll et al., 1990, 1996; Li et al., 1994). Further variability results from alternative splicing of NCX1, and tissue-specific variants have been identified and called NaCa1, NaCa2, . . . , NaCan (Kofuji et al., 1994; Lee et al., 1994). Pancreatic islets, purified β-cells, and RINm5F cells all express the isoforms NaCa3 and NaCa7, whereas the heart expresses NaCa1 (Kofuji et al., 1994; Lee et al., 1994; Van Eylen et al., 1997). (A new terminology has been proposed to designate NCX1 isoforms as NCX1 followed by a number to indicate the splicing isoform. Hence NaCa1, NaCa3, and NaCa7 are referred to as NCX1.1, NCX1.3, and NCX1.7, respectively (Quednau et al., 1997).) The heart and the β-cell isoforms of the exchanger show 94% and 96% identity, respectively.

Here we have used the combined whole-cell configuration of the patch-clamp technique and microfluorimetry to investigate whether the Na/Ca exchange is activated during β-cell electrical activity, to estimate its contribution to [Ca^{2+}]$_i$-removal, and to determine the extent to which electrical activity may be shaped by the operation of the exchanger.

MATERIALS AND METHODS

Cell preparation

Mouse pancreatic islets were isolated from NMRI mice (Alab, Sollentuna, Sweden; Bomholtgård, Ry, Denmark; or IFFA CREDO, Brussels, Belgium). The mice were stunned by a blow against the head and killed by cervical dislocation, and the pancreas was quickly removed and cut into small pieces. Pancreatic islets were then isolated by collagenase digestion. Single cells were prepared by shaking in Ca^{2+}-free medium essentially as previously described (Rorsman and Trube, 1986). Isolated cells were then plated on glass coverslips (for microfluorimetry) or Petri dishes and kept in tissue culture for up to 2 days in RPMI 1640 culture medium supplemented

with 5 mM glucose, fetal calf serum (Sigma, St. Louis, MO; 10% by volume), 100 μg/ml streptomycin, and 100 IU/ml penicillin. Experiments on glucose-stimulated β-cell electrical activity were carried out on freshly isolated intact pancreatic islets as previously described (Renström et al., 1996).

Electrophysiology

Whole-cell Ca^{2+} currents were recorded in the perforated patch whole-cell configuration (Horn and Marty, 1988) of the patch-clamp technique (Hamill et al., 1981). Na/Ca-exchange current-voltage (I-V) relationships were recorded in the conventional whole-cell configuration. All experiments were made using an EPC-7 patch-clamp amplifier (Heka Electronics, Lambrecht, Germany), except the recordings of Fig. 6 A, which were made using an EPC9 patch clamp (Heka Electronics, Pfalz). The current signal was filtered at 0.5–2 kHz and digitized at 1–4 kHz, using the programs pClamp (versions 5.5 and 6.0; Axon Instruments, Burlingame, CA) or pulse (version 7.89; Heka Electronics) in conjunction with a Labmaster (Axon Instruments) or ITC-16 AD/DA converters (Instrutech, New York, NY), respectively, and stored in a computer pending later analysis. Current-clamp recordings were made using the perforated patch whole-cell configuration, and the voltage signal was filtered at 500 Hz and sampled at 1 kHz.

Fluorescence measurements

Cytosolic Ca^{2+} was measured by dual-wavelength fluorimetry, using fura-2 (Molecular Probes, Eugene, OR), and recorded at video rate (25 samples/s) with an IonOptix imaging system (IonOptix Corp., Milton, MA) as described elsewhere (Bokvist et al., 1995). Excitation was set at 340/380 nm, and emission was recorded at 510 nm. Before the experiments, the cells were loaded with 0.2 μM fura-2 AM for 20 min. The fluorescence signal was calibrated by dialyzing cells with various Ca^{2+}/EGTA buffers with known $[Ca^{2+}]_i$ values. The K_d value was then obtained by fitting these data to the equation of Grynkiewicz et al. (1985).

Solutions

The standard extracellular solution was composed of (in mM) 138 NaCl, 5.6 KCl, 2.6 $CaCl_2$, 1.2 $MgCl_2$, 5 glucose, and 5 HEPES (pH 7.40 with NaOH). In the Na^+-free solutions NaCl was replaced by either 138 mM choline-Cl or 237.4 mM sucrose. The replacement of NaCl with sucrose resulted in the development of a positive liquid junction potential of ~20 mV (i.e., the voltage was −50 mV when the amplifier reported −70 mV). All voltages quoted in this paper have been corrected for this shift. To block voltage-gated Ca^{2+} currents, the extracellular medium was supplemented with 20 μM nifedipine in the experiments determining the I-V properties of the exchanger. In the latter experiments, the pipette solution consisted of (in mM) 95 CsCl, 30 NaCl, 1 $MgCl_2$, 5 HEPES (pH 7.35 with CsOH), 3 MgATP, 10 EGTA, and 9.75 or 10 $CaCl_2$. The intracellular pH was adjusted to 7.35 to increase the activity of the exchanger (see Plasman and Herchuelz, 1992). The free Ca^{2+} resulting from these Ca^{2+}/EGTA mixtures was determined as 3.5 μM and 14 μM by direct measurements in 3-ml aliquots of the pipette solution, using the Ca^{2+}-indicator BTC (Molecular Probes) and a spectrophotometer (LS-50B; Perkin-Elmer, Buckinghamshire, England). In some experiments, the pipette also contained XIP (exchange inhibitory peptide) (Li et al., 1991), synthesized as previously described (Van Eylen et al., 1994).

To estimate the net current attributable to the operation of the Na/Ca exchanger (Figs. 3 and 4), the current responses evoked by voltage ramps in the complete absence of extra- and intracellular Na^+ (to eliminate both the forward and reverse mode operations) were subtracted from those recorded under the control conditions.

In the perforated patch experiments the pipette solution consisted of (in mM) 81 Cs_2SO_4, 10 KCl, 1 $MgCl_2$, and 5 HEPES-KOH; 0.24 μg/ml amphotericin B (Sigma) was included in the pipette solution to establish

electrical contact with the cell interior. The extracellular medium used for the recordings of electrical activity from intact islets consisted of (in mM) 140 NaCl, 3.6 KCl, 0.5 NaH_2PO_4, 2 $NaHCO_3$, 2.5 $CaCl_2$, 5 HEPES, and 11 glucose (pH set at 7.4 with NaOH). Sodium was replaced by equimolar amounts of choline chloride where indicated. Similar data were observed in the absence or the presence of atropine (10 μM) to avoid any potential cholinergic effects of choline. The contribution of endoplasmic reticulum Ca^{2+}-ATPase (SERCA) to the overall Ca^{2+} buffering was assessed by inhibiting its operation by pretreatment with 0.5 μM thapsigargin (Alomone, Jerusalem, Israel) for 20 min.

Mathematical model

For the modeling of β-cell electrical activity we have used the deterministic model for β-cell bursting by Sherman et al. (1988). This model contains three ionic currents: delayed rectifying K^+ channels (I_{KDr}), voltage-dependent Ca^{2+} channels (I_{Ca}), and Ca^{2+}-activated high-conductance K^+ channels (I_{KCa}). We have inserted the necessary parameters describing the Na/Ca exchange current ($I_{Na/Ca}$) into this model. Thus, using Kirchoff's laws, the membrane potential (V_m) satisfies the equation

$$C_m \cdot \frac{dV_m}{dt} = -I_{KDr} - I_{Ca} - I_{KCa} - I_{Na/Ca} \qquad (1)$$

where

$$I_{Na/Ca} = C_m \cdot \bar{g}_{Na/Ca} \cdot \left(\frac{([Ca^{2+}]_i)^n}{([Ca^{2+}]_i)^n + K_{1/2}^n} \right) \cdot (V_m - V_{Na/Ca}) \qquad (2)$$

and

$$V_{Na/Ca} = \frac{R \cdot T}{F} \cdot \left(3 \cdot \ln \frac{[Na^+]_o}{[Na^+]_i} - \ln \frac{[Ca^{2+}]_o}{[Ca^{2+}]_i} \right) \qquad (3)$$

The Ca^{2+} affinity constant ($K_{1/2}$), the Hill coefficient (n), and the normalized whole-cell Na/Ca exchange conductance ($\bar{g}_{Na/Ca}$) in Eq. 2 were set at 1.5 μM, 5, and 44 pS/pF. These values produced the best fit to our experimental data. Ideally, the parameters in Eq. 2 should reflect the biophysical properties of the Na/Ca exchange in the β-cell. However, steep $[Ca^{2+}]_i$ gradients develop in the β-cell during Ca^{2+} entry through the voltage-gated Ca^{2+} channels, and the fura-2 measurements report only the average of the entire cell (cf. Bokvist et al., 1995). The submembrane Ca^{2+} concentration sensed by the Na/Ca exchange is accordingly likely to be severalfold higher than that indicated by the $[Ca^{2+}]_i$ recordings. As a consequence, when fitting Na/Ca exchange activity to the average $[Ca^{2+}]_i$ levels detected with fluorometry, the resulting Ca^{2+} affinity ($K_{1/2}$) and cooperativity coefficient (n) will also reflect the diffusion gradients in the cell. The $K_{1/2}$ value of 1.5 μM should therefore be understood as reflecting a much higher affinity constant of the exchange protein. However, it should be kept in mind that the mathematical models we have used operate with average $[Ca^{2+}]_i$. To provide the best possible coupling between model parameters and experimental data, we have chosen to correlate exchanger activity with average $[Ca^{2+}]_i$, i.e., the data underlying Fig. 1. The Na/Ca exchange permeability ($\bar{g}_{Na/Ca}$) was estimated from the data in Fig. 3, yielding a value of 44 pS/pF.

Considering that the Na/Ca exchanger is a Ca^{2+} transport protein, the exchange current also has to be included in the equation describing the Ca^{2+} balance in the cytoplasm:

$$\frac{d[Ca^{2+}]_i}{dt} = f \cdot (-\alpha \cdot (I_{Ca} - 2 \cdot I_{Na/Ca}) - k_{Ca} \cdot [Ca^{2+}]_i) \qquad (4)$$

where f is the fraction of free Ca^{2+} in the cytoplasm, α is a factor for converting current to change in cytosolic concentration per time unit, and k_{Ca} is a parameter that describes the β-cell Ca^{2+} removal. When modified as noted above, the set of equations of Sherman et al. (1988) was used for our simulations. Furthermore, the (fixed) parameters were set at the values
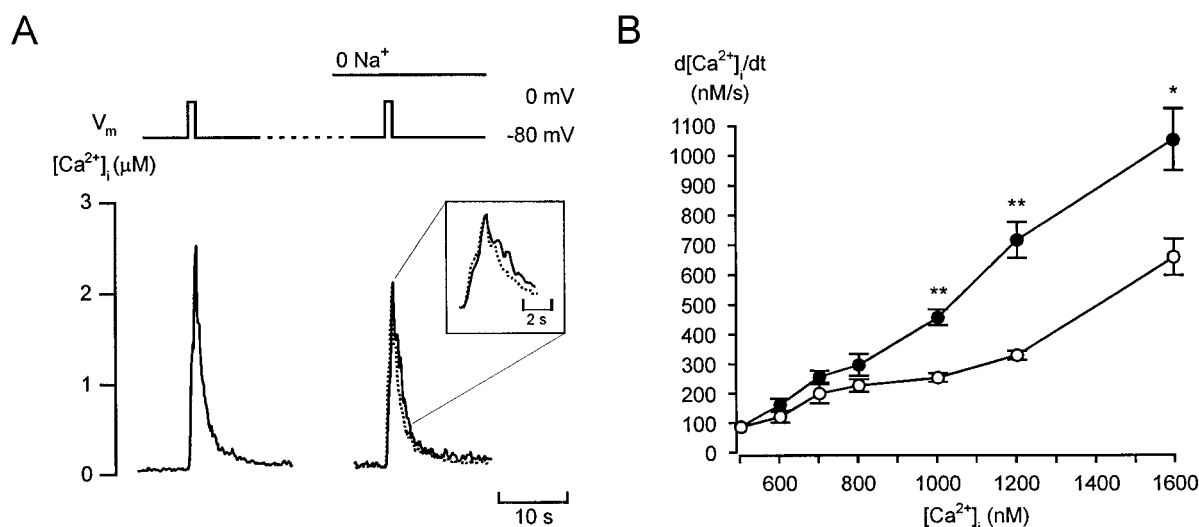
FIGURE 1   Removal of extracellular sodium reduces the rate of Ca^{2+} removal. (*A*) Calcium transients resulting from a 2-s depolarization from a holding potential of -80 to 0 mV in the presence (*left*) and the absence (*right*) of extracellular Na^{+} (replacement by sucrose). To facilitate comparison, the time course of the $[Ca^{2+}]_i$ transient in the presence of Na^{+} is shown as a dotted line and superimposed on the $[Ca^{2+}]_i$ transient observed in the absence of Na^{+}. Peak $[Ca^{2+}]_i$, the time constant for the recovery of $[Ca^{2+}]_i$, and basal $[Ca^{2+}]_i$ in this experiment were 2.7 μM, 2.3 s, and 0.16 μM versus 2.5 μM, 2.8 s, and 0.19 μM in the presence and absence of extracellular Na^{+}, respectively. (*Inset*) Recovery of the Ca^{2+} transient shown in an expanded time scale. (*B*) $[Ca^{2+}]_i$ recovery rates, $d[Ca^{2+}]_i/dt$, at various $[Ca^{2+}]_i$ levels in the presence (*filled circles*) and absence (replacement by sucrose; *empty circles*) of extracellular Na^{+}. Data are mean values $\pm$ SEM for five different experiments. **$p < 0.01$.

used by Sherman et al. (1988), with the exception of the parameters pertaining to the Na/Ca exchange. The equations of our model were solved numerically, using a variant of the Runge-Kutta method implemented in the NAG library (Numerical Algorithms Group, Downers Grove, IL). Computations were performed on an SGI R10000 workstation (Silicon Graphics, Mountain View, CA).

Data analysis

Exponential functions were fitted to the data points by the least-squares method ($[Ca^{2+}]_i$) or a Levenberg-Marquardt algorithm (tail currents). The $[Ca^{2+}]_i$ removal rates in Figs. 1 *B* and 5 were determined as the linear slope within ±0.2–0.4-μM intervals of $[Ca^{2+}]_i$. To compensate for variations in cell size, current amplitudes have been normalized against cell capacitance. Data are presented as mean values $\pm$ SEM. Statistical significances were evaluated using Student's *t*-test for paired (Figs. 1, 2, and 6) or unpaired (Figs. 3–5) data.

RESULTS

Na^{+} dependence of Ca^{2+} removal

Fig. 1 *A* shows the $[Ca^{2+}]_i$ transients induced by 2-s depolarizations from -80 mV to 0 mV in the presence (*left*) and absence (*right*) of external Na^{+}. Removal of Na^{+} decreased the rate of Ca^{2+} removal ($d[Ca^{2+}]_i/dt$). The removal rates at different $[Ca^{2+}]_i$ were estimated from the linear slope of the falling phase of the $[Ca^{2+}]_i$ transient around each $[Ca^{2+}]_i$ level of interest. This procedure could not be applied to $[Ca^{2+}]_i$ levels above 1.6 μM, and to estimate the removal rate at higher $[Ca^{2+}]_i$, a single exponential was fitted to the decay phase of the $[Ca^{2+}]_i$ transient. This procedure yielded time constants of 2.0 ± 0.2 s and 2.6 ± 0.2 s in the presence and absence of extracellular Na^{+} ($p < 0.01$, $n = 6$), respec-

tively. These mean values for the time constants correspond to initial removal rates (at the peak of the $[Ca^{2+}]_i$ transient estimated from $d[Ca^{2+}]_i/dt$ at $t = 0$) of 2200 and 1400 nM/s; the higher value is the removal rate in the presence of Na^{+}. This difference cannot be attributed to the peak $[Ca^{2+}]_i$ being different, because removal of Na^{+} had no statistically significant effect on the amplitude of the $[Ca^{2+}]_i$ transients (4.3 ± 1.9 μM and 3.8 ± 1.0 μM in the absence and presence of Na^{+}, respectively; $n = 6$). Indeed, the removal rates were lower in the absence than in the presence of Na^{+} at all $[Ca^{2+}]_i \geq 1$ μM (Fig. 1 *B*). The removal of Na^{+} had no statistically significant effect on basal $[Ca^{2+}]_i$ (0.19 ± 0.03 and 0.25 ± 0.05 μM in presence and absence of Na^{+}, respectively).

Slow Na^{+}-dependent tail currents reflect the operation of the Na-Ca exchanger

In heart cells, the Na/Ca exchanger has been reported to be electrogenic, with a stoichiometry of three Na^{+} for one Ca^{2+} (Kimura et al., 1987; Ehara et al., 1989). When the exchanger operates in the forward mode, each cycle will consequently be associated with the net uptake of one positive charge and thereby gives rise to an inward current ($I_{Na/Ca}$). Inward tail currents, attributable to the operation of the exchanger, have been observed in smooth muscle and cardiac cells after a depolarization (Beuckelmann and Wier, 1989; Zhou and Lipsius, 1993; McCarron et al., 1994). Fig. 2 illustrates the tail current observed after a 2-s depolarization from -80 to 0 mV in a single β-cell. In the presence of external Na^{+}, there is both a rapid and a slow component of
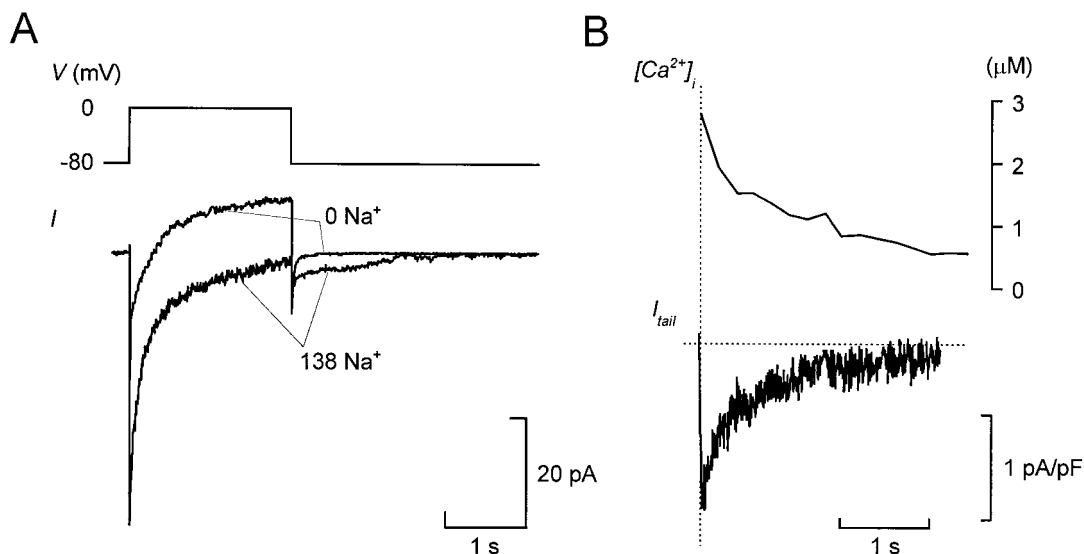
FIGURE 2   Whole-cell currents resulting from Ca^{2+} extrusion. (*A*) Whole-cell Ca^{2+} currents recorded in the perforated patch configuration in response to 2-s stimulations to 0 mV from a holding potential of -80 mV. Shown are the currents in the presence and absence of extracellular Na^+ (replacement by sucrose). Note the slow tail current (amplitude 3–4 pA) after the depolarization in the presence of Na^+. (*B*) Time course of $[Ca^{2+}]_i$ recovery and the Na^+-dependent tail current. Traces represent the average data of six experiments in which Na^+ had been replaced by sucrose.

the tail current. Removal of external Na^+ selectively abolished the slow component, whereas the rapid part (presumably reflecting the rapid closure of the L-type Ca^{2+} channels) was unaffected. In this cell, the slow Na^+-dependent tail current component had an amplitude of 4 pA. The slow tail current reappeared upon reintroduction of Na^+ into the extracellular medium (not shown). Interestingly, the time course of this Na^+-dependent tail current component paralleled the recovery of the $[Ca^{2+}]_i$ increase elicited by the voltage-clamp depolarization. Fig. 2 *B* shows the average of the $[Ca^{2+}]_i$ traces and the corresponding Na^+-dependent tail currents from the six experiments in which external Na^+ had been replaced by sucrose. Similar observations were made when Na^+ was replaced by choline (not shown). The integrated tail current amounted to 1.5 ± 0.2 pC/pF in the presence of Na^+ and fell to 0.7 ± 0.1 pC/pF when extracellular Na^+ was replaced by sucrose or choline ($p < 0.001$; $n = 18$). We attribute the difference, 0.8 ± 0.2 pC/pF, to the net charge carried by the exchanger.

Voltage-dependent operation of the Na/Ca exchanger

The current-voltage relationship of the Na/Ca exchange current is investigated in Fig. 3. For this series of experiments, $[Ca^{2+}]_i$ was buffered at 14 μM to activate the exchanger. Experiments were conducted using Cs^+-filled electrodes, and nifedipine was included in the bath solution to suppress voltage-dependent K^+- and L-type Ca^{2+} currents. The *I-V* relationships were obtained by ramping the membrane potential between -70 mV and $+30$ mV. The ramps were applied under control conditions (*black*) and after the replacement of Na^+ with choline or sucrose

(*dashed traces* in Fig. 3, *A* and *B*). It is clear that, regardless of whether Na^+ was replaced by choline or sucrose, the *I-V* relationship is flatter in the absence than in the presence of Na^+. The same effect was obtained when the exchange inhibitory peptide (XIP) (Li et al., 1991) was dialyzed into the cell interior at a final concentration of 10 μM (Fig. 3 *C*). These data are summarized in Fig. 3 *D*, where the net Na^+-dependent or XIP-sensitive currents for the different experimental conditions are displayed. The *I-V* relationships are essentially linear and reverse at ~-20 mV.

The amplitude of the currents, measured at a membrane voltage of -70 mV, were 3.9 ± 0.3 pA/pF under control conditions ($n = 21$), 2.0 ± 0.2 pA/pF after replacement of Na^+ with sucrose ($p < 0.001$ versus control; $n = 16$), 1.5 ± 0.2 pA/pF when choline was substituted for Na^+ ($p < 0.001$; $n = 13$), and 1.7 ± 0.1 pA/pF when the operation of the exchanger was inhibited by 10 μM XIP ($p < 0.001$; $n = 16$). Thus the Na^+-dependent component accounts for 1.9–2.4 pA/pF. The observed dependence on external Na^+, taken together with the action of XIP, constitutes good evidence for voltage-dependent operation of the exchanger in pancreatic β-cells.

Effects of extra- and intracellular Ca^{2+} on $I_{Na/Ca}$

Assuming that the β-cell Na/Ca exchanger operates with a stoichiometry of 3Na:1Ca, as in myocytes (Kimura et al., 1987; Ehara et al., 1989), the reversal potential ($E_{Na/Ca}$) of the exchanger is given by the equation

$$E_{Na/Ca} = 3 \cdot E_{Na} - 2 \cdot E_{Ca} \qquad (5)$$

where E_{Ca} and E_{Na} denote the Nernst potentials of Ca^{2+} and Na^+, respectively. Fig. 4 *A* shows the *I-V* relationships of

FIGURE 3 The Na/Ca exchanger *I-V* relationships. (*A*) Whole-cell currents recorded in the presence (*solid trace*) and absence (*dashed trace*) of extracellular Na^+ in response to a voltage ramp going from -70 to $+30$ mV. Na^+ was replaced by choline. (*B*) As in *A*, but Na^+ was replaced by sucrose. (*C*) As in *A*, but instead of removing external Na^+, we blocked the Na/Ca exchange by intracellular application of 10 μM XIP. (*D*) Net contribution of the Na/Ca exchanger obtained by subtracting the average *I-V* relationship obtained after inhibition of the exchanger (by replacement of extracellular Na^+ with choline$^+$ or sucrose or by inclusion of XIP in the pipette solution). Note the similarity of the *I-V* relationships. The curves shown represent the average of 21 (control), 16 (Na^+ replaced by sucrose), 13 (Na^+ replaced by choline$^+$), and 16 (XIP) cells.
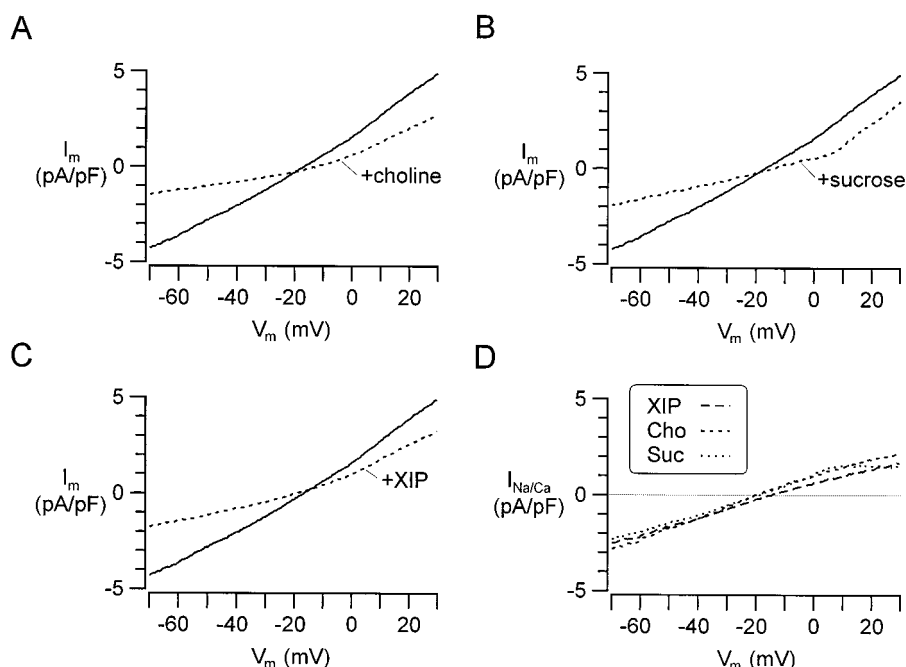
the Na/Ca exchanger recorded in the presence of 1, 1.6, 2.6, and 5 mM extracellular Ca^{2+}. The cytoplasmic Ca^{2+} concentration was buffered at 14 μM to (maximally) activate Na/Ca exchange. The observed reversal potentials at these different extracellular Ca^{2+} concentrations ($[Ca^{2+}]_o$) were 1, -9, -22, and -38 mV. The shift in $E_{Na/Ca}$ of 39 mV observed when $[Ca^{2+}]_o$ was increased from 1 to 5 mM agrees favorably with that expected theoretically (41 mV).

Fig. 4 *B* illustrates the influence of the intracellular Ca^{2+} concentration on the *I-V* relationship of the Na/Ca exchanger. Reducing $[Ca^{2+}]_i$ from 14 to 3.5 μM changed $E_{Na/Ca}$ from -22 to -53 mV. Again, this change of 31 mV is close to that predicted theoretically (36 mV) for a fourfold change in $[Ca^{2+}]_i$. Changing $[Ca^{2+}]_i$ also influenced the slope of the *I-V* relationship, and the normalized conductance fell from 53 to 12 pS/pF when $[Ca^{2+}]_i$ was lowered from 14 to 3.5 μM. This is consistent with the notion that $[Ca^{2+}]_i$ determines the activity of the Na/Ca exchanger in the pancreatic β-cell, as suggested by analogy to the situation in cardiac myocytes (Bridge, 1995).

Effects of the Ca^{2+}-ATPase inhibitor thapsigargin on $[Ca^{2+}]_i$ handling

Fig. 5 *A* shows the $[Ca^{2+}]_i$ transients induced by 2-s depolarizations from -80 mV to 0 mV under control conditions (*gray*) and after pretreatment (20 min) with 0.5 μM thapsigargin (*black trace*), an inhibitor of SERCA (Thastrup et al., 1990). Exposure of the β-cell to thapsigargin had pronounced effects on the rate of Ca^{2+} removal. The time constants for the recovery of $[Ca^{2+}]_i$ were 4.6 $\pm$ 0.7 s and 1.8 $\pm$ 0.25 s in the presence and absence of thapsigargin ($p < 0.01$, $n = 5$, in each group), respectively. Fig. 5 *B* shows the Ca^{2+} removal rate at different $[Ca^{2+}]_i$. In contrast

to the component of Ca^{2+} removal dependent on external Na^+, thapsigargin pretreatment had marked effects, even at $[Ca^{2+}]_i$ below 1 μM. Thapsigargin had only a slight effect on the amplitude of the $[Ca^{2+}]_i$ transient, and peak $[Ca^{2+}]_i$ increased from 0.9 $\pm$ 0.1 μM under control conditions to 1.2 $\pm$ 0.1 μM after inhibition of the Ca^{2+}-ATPase (values not statistically different).

β-Cell electrical activity

The effects of lowering (replacement by choline) extracellular Na^+ ($[Na^+]_o$) from 138 to 30 mM on glucose-induced electrical activity of a β-cell in an intact pancreatic islet are presented in Fig. 6. Reduction of the external Na^+ concentration had several effects on electrical activity, including membrane repolarization (affecting both the plateau and interburst voltage) and a shortening of both burst duration and the burst interval (Fig. 6 *A*). Expanded details of the electrical activity are shown in Fig. 6 *B*. The action on membrane potential is consistent with the Na/Ca exchanger giving rise to an inward current. Inhibition of the exchanger will remove this depolarizing influence, thus causing membrane repolarization. In a series of five experiments, the most negative membrane potential recorded in the interburst interval fell from -55 ± 4 to -60 ± 3 mV ($p < 0.025$), and the plateau potential hyperpolarized from -39 ± 4 to -44 ± 4 mV ($p < 0.01$) upon removal of Na^+. In addition, the spike amplitude increased from 26 $\pm$ 3 mV in the presence of Na^+ to 39 $\pm$ 3 mV in its absence ($p < 0.025$), and the burst duration was reduced from 16 $\pm$ 4 to 9 $\pm$ 2 s ($p < 0.05$). In addition, the interval between two successive bursts was reduced from 34 $\pm$ 4 s under control conditions to 12 $\pm$ 2 s ($p < 0.025$) in the absence of Na^+. The same results were obtained when Na^+ was replaced by choline in
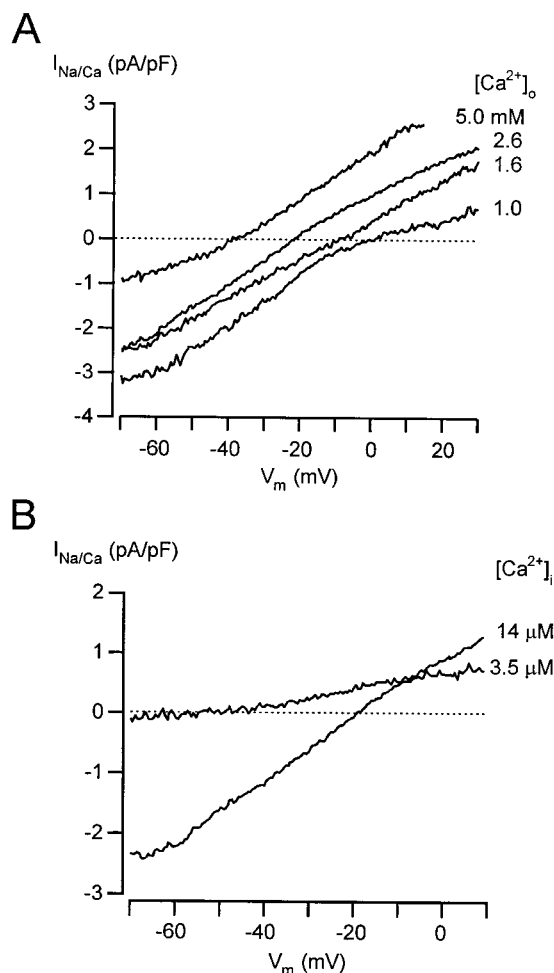
A

B

FIGURE 4   The influence of external and internal Ca^{2+} levels on the operation of the Na/Ca exchanger. (*A*) Net whole *I-V* relationships recorded at 1, 1.6, 2.6, and 5.0 mM extracellular Ca^{2+}. The traces shown are averages of 7 (1 mM), 7 (1.6 mM), 13 (2.6 mM), and 7 (5 mM Ca^{2+}) cells. Extracellular Na^+ was replaced with $choline^+$ to block the exchange current. (*B*) *I-V* curves recorded at 3.5 μM or 14 μM $[Ca^{2+}]_i$ with an external Ca^{2+} concentration of 2.6 mM. The curves represent the averages of 13 (14 μM) and 8 (3.5 μM Ca^{2+}) different cells.

A

B

FIGURE 5   Effects of thapsigargin on $[Ca^{2+}]_i$ buffering. (*A*) Calcium transients resulting from a 2-s depolarization from a holding potential of -80 to 0 mV under control conditions and after pretreatment of the β-cell for 20 min with 0.5 μM thapsigargin. To facilitate comparison, the $[Ca^{2+}]_i$ transient under control conditions is shown superimposed on the $[Ca^{2+}]_i$ transient observed in the presence of the ATPase inhibitor. Peak $[Ca^{2+}]_i$ and the time constant for the recovery of $[Ca^{2+}]_i$ in this experiment were 1.1 μM and 7.2 s versus 0.92 μM and 1.7 s in the presence and absence of thapsigargin, respectively. (*B*) $[Ca^{2+}]_i$ recovery rates, $d[Ca^{2+}]_i/dt$, at various $[Ca^{2+}]_i$ levels in the presence of thapsigargin (▼) and under control conditions (▲). Data are mean values ± SEM for five different experiments in each group. $*p < 0.05$; $**p < 0.025$.

the presence of atropine (10 μM). We can accordingly discard the possibility that the effects of substituting $choline^+$ for Na^+ are mediated by muscarinic receptors (cf. Hermans et al., 1987). Thus removal of external Na^+ in the presence of atropine reduced the burst duration from 12 ± 4 to 9 ± 3 s ($p < 0.05$; $n = 4$) and increased the interburst membrane potential potential ($-60 ± 5$ mV versus $-54 ± 6$ mV in control). A comparison of a burst in the presence of 140 Na^+ and a burst where $[Na^+]_o$ was lowered to 30 mM by replacement of Na^+ with choline in the presence of 10 μM atropine is shown in Fig. 6 *C*.

DISCUSSION

We have combined whole-cell configuration of the patch-clamp technique with microfluorimetry to characterize the biophysical properties of $I_{Na/Ca}$ in the insulin-secreting
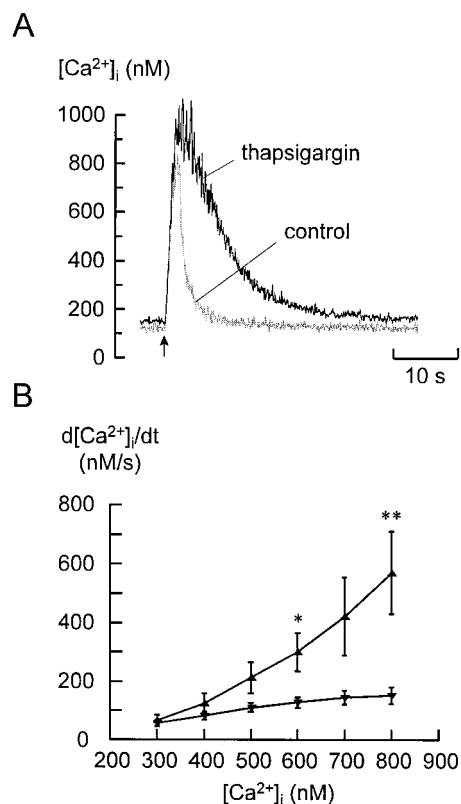
β-cell, its overall significance for the regulation of $[Ca^{2+}]_i$, and how it may influence glucose-induced electrical activity in pancreatic islets. Here we consider a few particularly interesting aspects of this work.

The Na/Ca exchanger participates in the regulation of $[Ca^{2+}]_i$

This study provides direct evidence for Na^+-dependent and electrogenic extrusion of Ca^{2+} in voltage-clamped mouse pancreatic β-cells. This component of Ca^{2+} removal becomes significant when $[Ca^{2+}]_i$ rises above 1 μM. The observation that the contribution of the Na^+-dependent component of Ca^{2+} removal is not detectable at $[Ca^{2+}]_i$ below 1 μM argues that the Na/Ca exchanger does not participate in the maintenance of basal $[Ca^{2+}]_i$. This notion is in keeping with the reported low affinity of the exchanger for Ca^{2+} (Barcenas-Ruiz et al., 1987; Hilgemann et al., 1992). Furthermore, even at the end of a 2-s voltage-clamp

FIGURE 6   Effects of lowering extracellular Na^+ on glucose-induced electrical activity. (A) Current-clamp recording of electrical activity seen in the presence of 11 mM glucose before and after $[Na^+]_o$ is reduced from 140 to 30 mM (substitution by choline). The membrane potential recordings were taken from freshly (same day) isolated mouse islets of Langerhans. (B) Details of the voltage records marked in A. The thin horizontal lines denote the lowest interburst potential, the plateau potential during the burst, and the peak action potential under control conditions (Na^+ present). (C) Comparison of bursts of action potentials recorded from another islet at normal and reduced extracellular Na^+, where 10 μM atropine was added together with choline to inhibit any muscarinic responses elicited by choline.
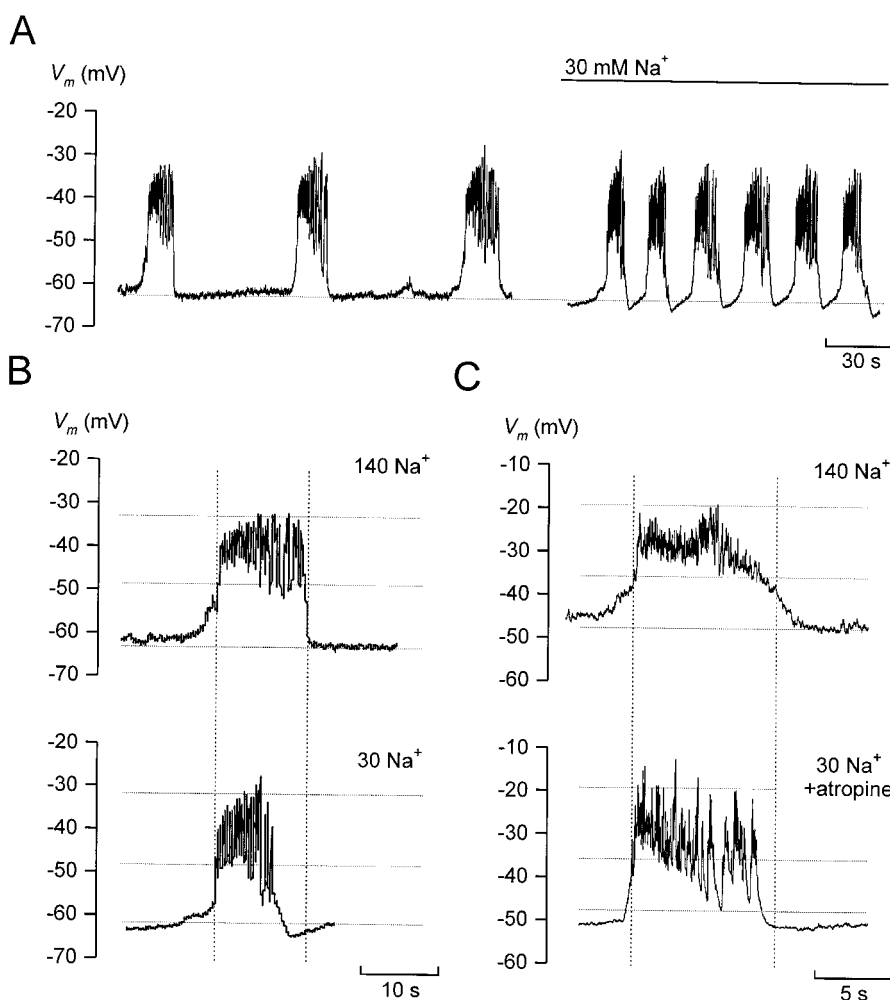
depolarization, when $[Ca^{2+}]_i$ exceeds 4 μM, the Na/Ca exchanger does not account for more than 36% of the Ca^{2+} removal rate. These considerations indicate that although the exchanger clearly participates in the restoration of $[Ca^{2+}]_i$, additional Ca^{2+}-buffering mechanisms with higher affinity for Ca^{2+} and capacity must also be operational (see below). In fact, it is even possible that our value for the contribution of the Na/Ca exchanger to the overall Ca^{2+} buffering represents an upper estimate. This would be the case if the exchanger were to start operating in the reverse mode after removal of extracellular Na^+ and mediating the uptake of Ca^{2+} into the cell rather than the extrusion. It seems, however, that we can discard this possibility. This is suggested by the following two observations: First, no consistent increase in $[Ca^{2+}]_i$ was observed upon replacing Na^+ with sucrose. Second, no significant changes in the amplitude of the depolarization-evoked $[Ca^{2+}]_i$ transients resulted from variations in the extracellular Na^+ concentration. These findings argue that reverse mode operation of the exchanger contributes negligibly to $[Ca^{2+}]_i$, even after removal of external Na^+. In contrast, on isolated mouse islets, Nadal et al. (1994) observed both increased basal $[Ca^{2+}]_i$ and larger $[Ca^{2+}]_i$ responses to K^+ depolarizations

in low extracellular Na^+ compared to normal Na^+ levels. However, in this study Li^+ was used as a replacement for Na^+, which causes a depolarization of the islet by 15–20 mV (cf. de Miguel et al., 1988). Consequently, these earlier observations may therefore reflect an increased Ca^{2+} influx through voltage-dependent Ca^{2+} channels due to the depolarization induced by replacing Na^+ with Li^+.

Relative contribution of Na^+- and ATP-driven Ca^{2+} uptake and extrusion mechanisms

Although the Na/Ca exchanger contributes to Ca^{2+} buffering, particularly at high $[Ca^{2+}]_i$, it is clear that additional Ca^{2+}-lowering mechanisms must be operational in the β-cell. This study reinforces previous observations that intracellular Ca^{2+}-ATPases are important in this context. Contrary to what appears to be the case with the Na/Ca exchanger, the effects of inhibiting the endoplasmic reticulum Ca^{2+}-ATPase by using thapsigargin were already evident at submicromolar $[Ca^{2+}]_i$. At 0.6 and 0.8 μM $[Ca^{2+}]_i$, Ca^{2+}-ATPase accounted for 57% and 73% of the Ca^{2+} removal rate, respectively. It seems likely that the remainder

reflects the contribution of the Ca^{2+}-ATPase of the plasma membrane or, possibly, the mitochondria (Park et al., 1996). However, we emphasize that the relative contribution of the exchanger and SERCA may be more significant in β-cells from other species. This is suggested by the interspecies variation in other tissues. For example, whereas the exchanger accounts for 7% of the total Ca^{2+} removal rate in rat myocytes, the corresponding values in the rabbit, ferret, and guinea pig range between 25% and 30% (Bers, 1991). In fact, we recently observed that Na/Ca exchange activity, measured as intracellular Na^+-dependent extracellular $^{45}Ca^{2+}$ uptake, and mRNA levels are 50% lower in mouse compared to rat pancreatic islets (Van Eylen et al., 1998).

The Na/Ca exchanger is electrogenic

A Na^+-dependent mode of Ca^{2+} extrusion has previously been described in voltage-clamped pancreatic β-cells, but the voltage dependence of its operation was not apparent (Rorsman et al., 1992). The present study reveals that the Na/Ca exchanger is influenced by the membrane potential and that it may operate in both the forward and reverse modes. The changes in reversal potential obtained upon variations of the extra- and intracellular Ca^{2+} concentrations are perfectly consistent with a $3Na^+$:$1Ca^{2+}$ stoichiometry, as has previously been documented for the exchanger in heart cells (Reeves and Hale, 1984; Kimura et al., 1987; Ehara et al., 1989). Moreover, the β-cell Na/Ca exchanger is inhibited by XIP at concentrations comparable to those that are effective in the heart cells (Chin et al., 1993). These biophysical and biochemical similarities between the β-cell and cardiac Na/Ca exchangers are not surprising, given that the isoforms present in the β-cell (NaCa3 and NaCa7) and in the heart (Na/Ca1) are the products of the same NCX1 gene (Kofuji et al., 1994; Lee et al., 1994, Van Eylen et al., 1997).

The Na/Ca exchanger shapes β-cell electrical activity

The glucose-induced electrical activity of the pancreatic β-cell is the result of a complex interplay between a number of voltage-dependent and voltage-independent membrane currents (review: Ashcroft and Rorsman, 1989; Henquin and Meissner, 1984). An understanding of how this electrical activity is generated is essential, given that it is tightly coupled to insulin secretion (Martin et al., 1997). The present observations that the operation of the Na/Ca exchanger is electrogenic and generates an inward current at membrane potentials more negative than -50 mV when $[Ca^{2+}]_i$ is elevated to high concentrations (>3.5 μM; Fig. 4 B) suggest that it may influence the electrical activity of the β-cell. At the more depolarized peak potentials of the spikes, the exchange is capable of running in the reverse mode, allowing Ca^{2+} to enter the cell. It should be pointed out that although the exchanger may thus mediate Ca^{2+}

uptake, available data are conflicting as to whether this actually takes place (compare Nadal et al., 1994, and Garcia-Barrado et al., 1996).

It is worth pointing out that the current resulting from the activity of the exchanger is very small, even under conditions that can be expected to produce maximum activation (14 μM intracellular $[Ca^{2+}]_i$); the whole-cell conductance (normalized against cell capacitance) attributable to the operation of the exchanger is $\sim$0.05 nS/pF (Fig. 3 D). This is little more than 1% of the whole-cell K_{ATP} conductance (4 nS/pF; Rorsman and Trube, 1985) and only $\sim$15% of the voltage-gated Ca^{2+} conductance (0.3 nS/pF; estimated from a peak Ca^{2+} current at 0 mV of 100 pA, a reversal potential at $+60$ mV, and a cell capacitance of 5 pF; Rorsman and Trube, 1986). However, it is a dangerous practice to extrapolate the functional significance of a conductance from the size of the current, and small currents may have great effects on the membrane potential, because the input resistance of the β-cell in the presence of glucose is very high ($\geq$1 GΩ). The elucidation of its effects on β-cell electrical activity is further complicated by the lack of a selective pharmacological inhibitor of the exchanger. The traditional approach to the influence of the Na/Ca exchanger on electrical activity is to omit extracellular Na^+ from the medium (cf. Ribalet and Beigelman, 1982). However, this protocol is fraught with many problems. For example, other Na^+-dependent conductances will also be suppressed, and this is likely to affect the membrane potential of the cell, which in turn will influence the gating of voltage-gated currents. A further complication is that the reversal potential of $I_{Na/Ca}$ is not constant, and the direction of current flow (inward or outward) at a given membrane potential will vary with $[Ca^{2+}]_i$ (Fig. 4 B). However, the I-V properties of the Na/Ca exchanger and the effects of omitting extracellular Na^+ suggest that the current generated by the exchanger does not participate in the termination of the burst. In contrast, at the plateau potential when $[Ca^{2+}]_i$ is high, it will produce an inward depolarizing current that rather tends to prolong the burst of action potentials. This behavior is obviously reminiscent of the situation prevailing during the cardiac action potential (Egan et al., 1989; Noble et al., 1991).

Mathematical modeling suggests glucose may increase electrical activity by increasing $I_{Na/Ca}$

To analyze the role(s) of the Na/Ca exchanger in the generation of β-cell electrical activity in greater detail, we have incorporated the biophysical properties of the exchanger into the deterministic model for β-cell bursting developed by Sherman et al. (1988). Details of the modification made to their model are outlined further in Materials and Methods. Similar results were obtained when the model of Keizer and Magnus (1989) was used. Here we focus on the results obtained with the former model. Examples of simulated β-cell electrical activity are shown in Fig. 7 A. The mathematical model correctly predicts the changes in electrical
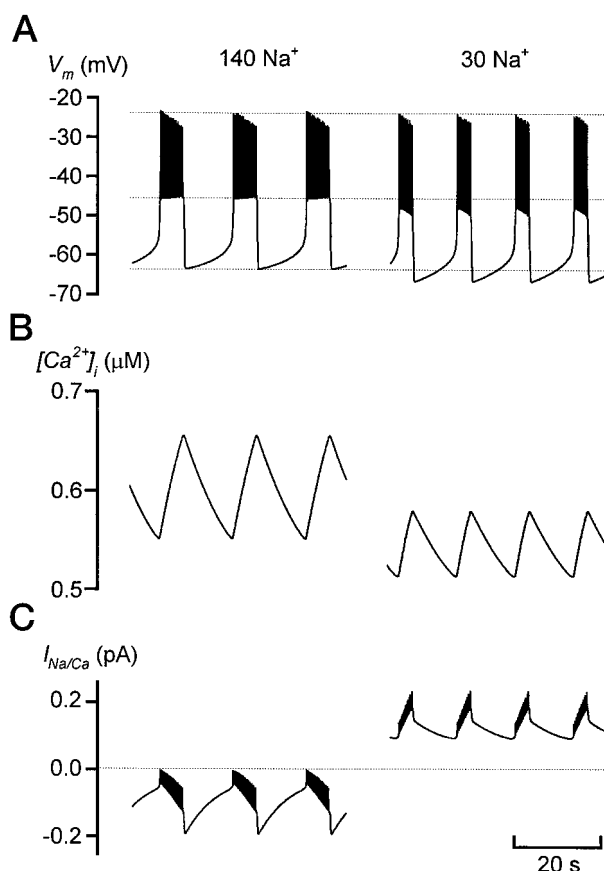
FIGURE 7 Computer simulations of electrical activity. (*A*) Influence of lowering extracellular Na$^+$ ([Na$^+$]$_o$) from 140 to 30 mM on simulated glucose-stimulated electrical activity. The model burst duration is reduced by 40% as a consequence of the changed [Na$^+$]$_o$ level. (*B*) Variations in model [Ca^{2+}]$_i$ levels in the presence of normal (*left*) and low extracellular Na$^+$ (*right*). (*C*) Corresponding currents carried by the Na/Ca exchange ($I_{Na/Ca}$) in the model cell. Observe that $I_{Na/Ca}$ during the burst changed from an inward depolarizing current in normal [Na$^+$]$_o$ to an outward current in low [Na$^+$]$_o$.

activity induced by lowering extracellular Na$^+$ that are observed experimentally. However, the interburst duration experimentally is reduced by ~50%, whereas only a 5% change is expected from the model. This discrepancy should be considered against the fact that 1–2 s after the termination of a burst (cf. Figs. 1 and 2), [Ca^{2+}]$_i$ will drop below the concentration required for activation of the Na/Ca exchanger. Most of the consequences of Na$^+$ removal for the interburst interval are therefore likely to involve effects other than inhibition of the exchanger. For example, the reduction of [Na$^+$]$_i$ that is likely to follow upon omission of extracellular Na$^+$ leads to a decreased activity of the Na$^+$/K$^+$-ATPase, which, via an increased ATP/ADP ratio (Grapengiesser et al., 1993), translates into closure of the K$_{ATP}$ channels and membrane depolarization. Indeed, long exposures of the cells to low [Na$^+$]$_o$ lead to a gradual increase in the membrane potential and ultimately continuous electrical activity (data not shown, but see Ribalet and Beigelman, 1982). Here we have kept the duration of Na$^+$ removal to a

minimum to avoid, as much as is possible, the influence of Na$^+$/K$^+$ pump inhibition on our data.

Both the model by Sherman et al. (1988) and that of Keizer and Magnus (1989) postulate a [Ca^{2+}]$_i$-dependent termination of the burst, either by activation of the large-conductance Ca^{2+}-activated K$^+$ channel (Sherman et al., 1988) or by [Ca^{2+}]$_i$-dependent modulation of the ATP-regulated K$^+$ channel (Keizer and Magnus, 1989). As a consequence, it is important to examine the effects of Na$^+$ removal on [Ca^{2+}]$_i$ in the model. In the presence of 30 mM Na$^+$, [Ca^{2+}]$_i$ is lower than at 140 mM external Na$^+$ (Fig. 7 *B*). Consequently, the shortening of the bursts predicted by the models cannot simply be attributed to an increased activity of Ca^{2+}-dependent K$^+$ currents. It may seem paradoxical that the reversal of the exchange (i.e., removing a Ca^{2+} extrusion mechanism) leads to reduced [Ca^{2+}]$_i$ levels. However, it should be kept in mind that whereas the exchanger gives rise to an inward current at normal Na$^+$, the current flow is outward at low Na$^+$, thus repolarizing the β-cell (cf. Fig. 7 *C*). At the more negative interburst potential resulting from the changed exchanger activity, the voltage-dependent Ca^{2+} influx through L-type Ca^{2+} channels in the model of Sherman et al. will be reduced, which in turn leads to lower basal [Ca^{2+}]$_i$. In addition, the shorter burst duration in 30 mM Na$^+$ (resulting from the premature termination of spiking due to the operation of the exchanger) will lead to a lower total Ca^{2+} influx compared to what occurs at 140 mM Na$^+$ and, consequently, a smaller Ca^{2+} build-up during the burst.

The effects of Na$^+$ removal on burst duration and the interburst potential are easiest to understand if the exchanger normally produces an inward current that depolarizes the β-cell and extends the duration of the plateau phase. As already pointed out, this makes it unlikely that the exchanger is involved in the termination of the bursts, but this does not exclude the possibility that it modulates its duration. For example, an experimental condition resulting in an elevation of the intracellular Na$^+$ concentration ([Na$^+$]$_i$), such as that occurring in response to stimulation of the β-cell with acetylcholine (Gilon and Henquin, 1993; Miura et al., 1996), can be expected to result in a shortening of the burst (Fig. 8). Conversely, a reduction of [Na$^+$]$_i$ can
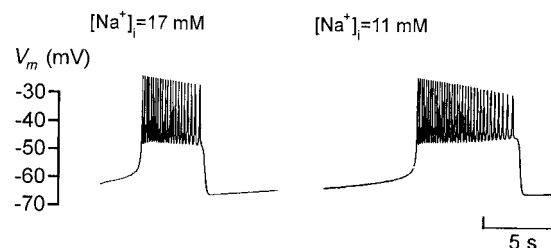

FIGURE 8 Computer simulations of the impact of changes in the intracellular Na$^+$ level ([Na$^+$]$_i$) on the β-cell bursting pattern. Bursts of action potentials in the presence of normal extracellular Na$^+$ and [Na$^+$]$_i$ were set to 17 mM (*left*). The reduction of intracellular Na$^+$ from 17 to 11 mM (*right*) led to a 60% increase in burst duration.

be expected to produce the opposite effect and prolong the burst. In this context it is pertinent that glucose has been reported to lower $[Na^+]_i$ in pancreatic β-cells (Saha and Grapengiesser, 1995). It is therefore tempting to speculate that this translates, via an increased activity of the exchanger, into prolonged bursts of action potentials. Thus the concentration-dependent glucose-induced stimulation of electrical activity may reflect the combined effects of the sugar on K_{ATP}-channel activity and the Na/Ca exchanger. Furthermore, the activity of the exchanger in squid axons, guinea pig myocytes, and rat β-cells is dependent on access to intracellular ATP (DiPolo and Beaugé, 1991; DiPolo and Beaugé, 1994; Hilgemann, 1990; Hilgemann et al., 1991; Haworth and Goknur, 1996; Plasman and Herchuelz, 1992). The cytoplasmic ATP/ADP ratio increases dramatically after glucose stimulation (Detimary et al., 1996), and there is evidence that these changes are particularly pronounced in the submembrane space, i.e., the milieu to which the Na/Ca exchanger is exposed (Niki et al., 1989). These changes, by increasing the current attributable to the exchanger, can be expected to promote electrical activity, thus ensuring an additional connection between the metabolic state of the β-cell and its membrane conductance(s).

REFERENCES

Ashcroft, F. M., and P. Rorsman. 1989. Electrophysiology of the pancreatic B-cell. *Prog. Biophys. Mol. Biol.* 54:87–143.

Atwater, I., C. M. Dawson, B. Ribalet, and E. Rojas. 1979. Potassium permeability activated by intracellular calcium ion concentration in the pancreatic beta cell. *J. Physiol. (Lond.).* 288:575–588.

Barcenas-Ruiz, L., D. J. Beuckelmann, and W. G. Wier. 1987. Sodium-calcium exchange in heart: membrane currents and changes in $[Ca^{2+}]_i$. *Science.* 238:1720–1722.

Bers, D. M. 1991. Species differences and the role of sodium-calcium exchange in cardiac muscle relaxation. *Ann. N.Y. Acad. Sci.* 639:375–385.

Beuckelmann, D. J., and W. G. Wier. 1989. Sodium-calcium exchange in guinea-pig cardiac cells: exchange current and changes in intracellular Ca^{2+}. *J. Physiol. (Lond.).* 414:499–520.

Bokvist, K., L. Eliasson, C. Ämmälä, E. Renström, and P. Rorsman. 1995. Co-localization of L-type Ca^{2+} channels and insulin-containing secretory granules and its significance for the initiation of exocytosis in mouse pancreatic B-cells. *EMBO J.* 14:50–57.

Bridge, J. H. B. 1995. Na-Ca exchange currents. *In* Cell Physiology Source Book. N. Sperelakis, editor. Academic Press, San Diego.

Chin, T. K., K. W. Spitzer, D. Philipson, and J. H. B. Bridge. 1993. The effect of exchanger inhibitory peptide on sodium-calcium exchange current in guinea pig ventricular cells. *Circ. Res.* 72:497–503.

Cook, D. L., W. E. Crill, and D. Porte. 1980. Plateau potentials in pancreatic islet cells are voltage-dependent action potentials. *Nature.* 286:404–406.

de Miguel, R., T. Tamagawa, W. Schmeer, M. Nenquin, and J. C. Henquin. 1988. Effects of acute sodium omission on insulin release, ionic flux and membrane potential in mouse pancreatic B-cells. *Biochim. Biophys. Acta.* 969:198–207.

Detimary, P., G. Van den Berghe, and J. C. Henquin. 1996. Concentration dependence and time course of the effects of glucose on adenine and guanine nucleotides in mouse pancreatic islets. *J. Biol. Chem.* 271:20559–10565.

DiPolo, R., and L. Beaugé. 1991. Regulation of Na-Ca exchange. An overview. *Ann. N.Y. Acad. Sci.* 639:100–111.

DiPolo, R., and L. Beaugé. 1994. Effects of vanadate on MgATP stimulation of Na-Ca exchange support kinase-phosphatase modulation in squid axons. *Am. J. Physiol.* 266:C1382–C1391.

Egan, T. M., S. J. Noble, T. Powell, A. J. Spindler, and V. W. Twist. 1989. Sodium-calcium exchange during the action potential in guinea-pig ventricular cells. *J. Physiol. (Lond.).* 41:639–661.

Ehara, T., S. Matsuoka, and A. Noma. 1989. Measurement of reversal potential of Na^+-Ca^{2+} exchange current in single guinea-pig ventricular cells. *J. Physiol. (Lond.).* 410:227–249.

Eisner, D. A., and W. J. Lederer. 1985. Na-Ca exchange stoichiometry and electrogenicity. *Am. J. Physiol.* 248:C189–C202.

Garcia-Barrado, M. J., P. Gilon, Y. Sato, M. Nenquin, and J. C. Henquin. 1996. No evidence for a role of reverse Na^+-Ca^{2+} exchange in insulin release from mouse pancreatic islets. *Am. J. Physiol.* 271:E426–E433.

Gilon, P., and J. C. Henquin. 1993. Activation of muscarinic receptors increases the concentration of free Na^+ in mouse pancreatic B-cells. *FEBS Lett.* 315:353–356.

Grapengiesser, E., A. Berts, S. Saha, P. E. Lund, E. Gylfe, and B. Hellman. 1993. Dual effects of Na/K pump inhibition on cytoplasmic Ca^{2+} oscillations in pancreatic beta-cells. *Arch. Biochem. Biophys.* 300:372–377.

Grynkiewicz, G., R. Y. Poenie, and R. Y. Tsien. 1985. A new generation of Ca^{2+} indicators with greatly improved fluorescence properties. *J. Biol. Chem.* 260:3440–3450.

Hamill, O. P., A. Marty, E. Neher, B. Sakmann, and F. Sigworth. 1981. Improved patch-clamp techniques for high-resolution current recording from cells and cell-free membrane patches. *Pflügers Arch.* 391(2):85–100.

Haworth, R. A., and A. B. Goknur. 1996. Regulation of sodium-calcium exchange in intact myocytes by ATP and calcium. *Ann. N.Y. Acad. Sci.* 779:464–479.

Henquin, J. C., and H. P. Meissner. 1984. Significance of ionic fluxes and changes in membrane potential for stimulus-secretion coupling in pancreatic B-cells. *Experientia.* 40:1043–1052.

Hermans, M. P., M. Bozem, R. de Miguel, and J. C. Henquin. 1987. Muscarinic effects of choline in mouse pancreatic B-cells. *Med. Sci. Res.* 15:1343–1344.

Hilgemann, D. W. 1990. Regulation and deregulation of cardiac Na-Ca exchange in giant excised sarcolemmal membrane patches. *Nature.* 344:242–245.

Hilgemann, D. W., A. Collins, D. P. Cash, and G. A. Nagel. 1991. Cardiac Na-Ca exchange system in giant membrane patch. *Ann. N.Y. Acad. Sci.* 639:126–139.

Hilgemann, D. W., A. Collins, and S. Matsuoka. 1992. Steady-state and dynamic properties of cardiac sodium-calcium exchange. Secondary modulation by cytoplasmic calcium and ATP. *J. Gen. Physiol.* 100:933–961.

Horn, R., and A. Marty 1988. Muscarinic activation of ionic currents measured by a new whole-cell recording method. *J. Gen. Physiol.* 92:145–159.

Keizer, J., and G. Magnus 1989. ATP-sensitive potassium channel and bursting in the pancreatic beta cell. *Biophys. J.* 56:229–242.

Kimura, J., S. Miyamae, and A. Noma 1987. Identification of sodium-calcium exchange in single ventricular cells of guinea-pig. *J. Physiol. (Lond.).* 384:199–222.

Kofuji, P., W. J. Lederer, and D. H. Schulze. 1994. Mutually exclusive and cassette exons underlie alternatively spliced isoforms of the Na/Ca exchanger. *J. Biol. Chem.* 269:5145–5149.

Lee, S.-L., A. S. L. Yu, and J. Lytton. 1994. Tissue-specific expression of Na$^+$-Ca^{2+} exchanger isoforms. *J. Biol. Chem.* 269:14849–14852.

Li, Z., S. Matsuoka, L. V. Hryshko, D. A. Nicoll, M. M. Bersohn, E. P. Burke, R. P. Lifton, and K. D. Philipson. 1994. Cloning of the NCX2 isoform of the plasma membrane Na$^+$-Ca^{2+} exchanger. *J. Biol. Chem.* 269:17434–17439.

Li, Z., D. A. Nicoll, A. Collins, D. W. Hilgemann, A. G. Filoteo, J. T. Penniston, J. N. Weiss, J. M. Tomich, and K. D. Philipson. 1991. Identification of a peptide inhibitor of the cardiac sarcolemmal Na$^+$-Ca^{2+} exchanger. *J. Biol. Chem.* 266:1014–1020.

Martin, F., J. Ribas, and B. Soria. 1997. Cytosolic Ca^{2+} gradients in pancreatic islet-cells stimulated by glucose and carbachol. *Biochem. Biophys. Res. Commun.* 235:465–468.

McCarron, J. G., J. V. Walsh, and F. S. Fay. 1994. Sodium/calcium exchange regulates cytoplasmic calcium in smooth muscle. *Pflügers Arch.* 426:199–205.

Miura, Y., P. Gilon, and J.-C. Henquin. 1996. Muscarinic stimulation increases Na$^+$ entry in pancreatic B-cells by a mechanism other than the emptying of intracellular Ca^{2+} pools. *Biochem. Biophys. Res. Commun.* 224:67–73.

Nadal, A., M. Valdeomillos, and B. Soria. 1994. Metabolic regulation of intracellular calcium concentration in mouse pancreatic islets of Langerhans. *Am. J. Physiol.* 267:E769–E774.

Nicoll, D. A., S. Longoni, and K. D. Philipson. 1990. Molecular cloning and functional expression of the cardiac sarcolemmal Na$^+$-Ca^{2+} exchanger. *Science.* 250:562–565.

Nicoll, D. A., B. D. Quednau, Z. Qui, Y.-R. Xia, A. J. Lusis, and K. D. Philipson. 1996. Cloning of the third mammalian Na$^+$-Ca^{2+} exchanger, NCX3. *J. Biol. Chem.* 271:24914–24921.

Niki, I., F. M. Ashcroft, and S. J. H. Ashcroft. 1989. The dependence on intracellular ATP concentration of ATP-sensitive K-channels and of Na,K-ATPase in intact HIT-T15 beta-cells. *FEBS Lett.* 257:361–364.

Noble, D., S. J. Noble, G. C. Bett, Y. E. Earm, W. K. Ho, and I. K. So. 1991. The role of the sodium-calcium exchange during the cardiac action potential. *Ann. N.Y. Acad. Sci.* 639:334–353.

Park, Y. B., J. Herrington, D. F. Babcock, and B. Hille. 1996. Ca^{2+} clearance mechanisms in isolated rat adrenal chromaffin cells. *J. Physiol. (Lond.).* 492:329–346.

Plasman, P.-O., and A. Herchuelz. 1992. Regulation of Na$^+$-Ca^{2+} exchange in the rat pancreatic B cell. *Biochem. J.* 285:123–127.

Quednau, B. D., D. A. Nicoll, and K. D. Philipson. 1997. Tissue specificity and alternative splicing of the Na$^+$/Ca^{2+} exchanger isoforms NCX1, NCX2, and NCX3 in rat. *Am. J. Physiol.* 272:C1250–C1261.

Reeves, J. P., and C. C. Hale. 1984. The stoichiometry of the cardiac sodium-calcium exchange system. *J. Biol. Chem.* 259:7733–7739.

Renström, E., W.-G. Ging, K. Bokvist, and P. Rorsman. 1996. Neurotransmitter-induced inhibition of exocytosis in insulin-secreting β cells by activation of calcineurin. *Neuron.* 17:513–522.

Ribalet, B., and P. M. Beigelman. 1982. Effect of sodium on β-cell electrical activity. *Am. J. Physiol.* 242:C296–C303.

Rorsman, P., C. Ämmälä, P.-O. Berggren, K. Bokvist, and O. Larsson. 1992. Cytoplasmic calcium transients due to single action potentials and voltage-clamp depolarizations in mouse pancreatic B-cells. *EMBO J.* 11:2877–2884.

Rorsman, P., and G. Trube. 1985. Glucose dependent K$^+$-channels in pancreatic β-cells are regulated by intracellular ATP. *Pflügers Arch.* 405:305–309.

Rorsman, P., and G. Trube. 1986. Calcium and delayed potassium currents in mouse pancreatic β-cells under voltage-clamp conditions. *J. Physiol. (Lond.).* 374:531–550.

Saha, S., and E. Grapengiesser. 1995. Glucose promotes turnover of Na$^+$ in pancreatic beta-cells. *Biochim. Biophys. Acta.* 1265:209–212.

Santos, R. M., and E. Rojas. 1989. Muscarinic receptor modulation of glucose-induced electrical activity in mouse pancreatic B-cells. *FEBS Lett.* 249:411–417.

Sherman, A., J. Rinzel, and J. Keizer. 1988. Emergence of organized bursting in clusters of pancreatic β-cells by channel sharing. *Biophys. J.* 54:411–425.

Thastrup, O., P. J. Cullen, B. K. Drøbak, M. R. Hanley, and A. P. Dawson. 1990. Thapsigargin, a tumor promoter, discharges intracellular Ca^{2+} stores by specific inhibition of the endoplasmic reticulum Ca^{2+}-ATPase. *Proc. Natl. Acad. Sci. USA.* 87:2466–2470.

Van Eylen, F., V. Duquesne, A. Bollen, and A. Herchuelz. 1998. Species specific transcription pattern and activity of Na/Ca exchange isoforms in pancreatic β-cells. *Diabetologia.* 41(Suppl. 1):A130.

Van Eylen, F., P. Gourlet, A. Vandermeers, P. Lebrun, and A. Herchuelz. 1994. Inhibition of Na/Ca exchange by Phe-Met-Arg-Phe-NH$_2$ (FM-RFa)-related peptides in intact rat pancreatic B-cells. *Mol. Cell. Endocrinol.* 106:R1–R5.

Van Eylen, F., M. Svoboda, and A. Herchuelz. 1997. Identification, expression pattern and activity of Na/Ca exchanger isoforms in rat pancreatic β-cells. *Cell Calcium.* 21:185–193.

Zhou, Z., and S. L. Lipsius. 1993. Na$^+$-Ca^{2+} exchange current in latent pacemaker cells isolated from cat right atrium. *J. Physiol. (Lond.).* 466:263–285.